Miriam Exner*, Patryk Szwargulski, Peter Ludewig, Tobias Knopp and Matthias Graeser

3D Printed Anatomical Model of a Rat for Medical Imaging

Abstract: For medical research, approximately 115 million animals are needed every year. Rodents are used to test possible applications and procedures for the diagnosis of anatomical and physiological diseases. However, working with living animals increases the complexity of an experiment. Accurate experimental planning is essential in order to fulfill the 3R rules (replace, reduce and refine). Especially in tracer-based imaging modalities, such as magnetic particle imaging (MPI), where only nanoparticles give a positive contrast, the anatomical structure of the rodent is not visible without co-registration with another imaging modality. This leads to problems in the experimental planning, as parameters, such as field of view, rodent position and tracer concentration, have to be determined without visual feedback. In this work, a 3D CAD rat model is presented, which can be used to improve the experiment planning and thus reduce the number of animals required. It was determined using an anatomy atlas and 3D printed with stereolithography. The resulting model contains the most important organs and vessels as hollow cavities. By filling these with appropriate tracer materials, the phantom can be used in different imaging modalities such as MPI, magnetic resonance imaging (MRI) or computed tomography (CT). In a first MPI measurement, the phantom was filled with superparamagnetic nanoparticles. Finally, a successful visualization of all organs and vessels of the phantom was possible. This enables the planning of the experiment and the optimization of experimental parameters for a region of interest, where certain organs in a living animal are localized.

Keywords: Rat Model, Magnetic Particle Imaging, 3D Printing

https://doi.org/10.1515/cdbme-2019-0048

***Corresponding author: Miriam Exner:** Section for Biomedical Imaging, University Medical Center Eppendorf, Hamburg, Germany; Institute for Biomedical Imaging, Technical University Hamburg, Hamburg, Germany, e-mail: miriam.exner@tuhh.de
Patryk Szwargulski, Tobias Knopp, Matthias Graeser: Section for Biomedical Imaging, University Medical Center Eppendorf, Hamburg, Germany; Institute for Biomedical Imaging, Technical University Hamburg, Hamburg, Germany
Peter Ludewig: Department of Neurology, University Medical Center Eppendorf, Hamburg, Germany

1 Introduction

Medical research requires the use of laboratory animals for toxological studies, pharmaceutical tests, tests of new medical procedures and showing the improvement of imaging technologies within a real case scenario. The total amount of used animals is unknown but estimated to be above 115 million per year worldwide [1]. 80 % of these are rodents (mice, rats, guinea-pigs) and rabbits [2]. Animal studies follow strict regulations to ensure the compliance with ethical rules. On the other hand, these rules increase the complexity as well as the necessary planning time of an experiment. Following the 3R rules (replace, reduce and refine) [3] by using a phantom instead of the animal, the experiment is not only more ethical but also simpler regarding the necessary effort. This requires that the phantom shares the same features as a living animal.

In this work, a 3D CAD model is presented, which mimics the main parts of the anatomy of a rat. With 14 %, rats are the second most frequently used experimental animals after mice [2]. The presented rat phantom can be used to improve the planning of *in vivo* experiments and thus reduce the burden for animal studies. The model was created in computer-aided design (CAD, SolidWorks, Dassault Systèmes, Vélizy-Villacoublay, France) based on an anatomy atlas of rats [4] and fabricated using additive manufacturing. It contains all essential organs and vessels, which are hollow and can be filled with different kinds of materials. This allows an anatomically close distribution of the tracer to be modeled. The model was evaluated using magnetic particle imaging (MPI). MPI images the distribution of superparamagnetic iron oxide (SPIO) nanoparticles using static and dynamic magnetic fields for excitation and spatial encoding. MPI combines a high spatial and temporal resolution as well as a high sensitivity. In addition, this modality enables the performance of real-time *in vivo* imaging [5]. For the MPI measurements, the cavities of the phantom were filled with a nanoparticle contrast agent at different concentrations. The model can be used for the exact planning and design of the imaging sequences as well as the position planning of the animal in the field of view (FOV). Thus, the number of animals required for a medical study can be reduced. Beside the model itself, the first MPI images of the model are presented.

2 Material and Methods

2.1 Model Design

The model creation was based on an anatomy atlas containing sagittal, coronal and transverse cut sections of rats [4]. Most of these rats are approximately 8 weeks old and weigh about 200 g. By measuring the dimensions and the shape of the main organs and vessels, an ordinary rat was modeled. Furthermore, the shape of some organs was modified based on MRI images of a mouse to better imitate the lying position of the rat during an experiment. The organs and vessels of the model were designed as hollow cavities with a wall thickness of at least 1 mm and can be filled individually. By selecting different tracer concentrations for the cavities, an organ-specific perfusion can be emulated. In order to facilitate the printing process and the subsequent post-processing, the brain, the heart as well as the spleen and the left kidney were created as individual parts separated from the other organs. In addition, the vessels were split into two parts, which can be joined after the printing process. The designed CAD model is shown in Figure 1a. The volumes of the individual organs and vessels are listed in Table 1.

2.2 3D Printing and Post-Processing

The organs and vessels of the model were fabricated with the stereolithography printer Form 2 (Formlabs GmbH, Berlin, Germany), which features a UV laser spot size of 140 µm and a layer height between 25 and 100 µm. The non-magnetic clear resin V4 (Formlabs GmbH, Berlin, Germany) was used as printing material. As required for the phantom, this technology enables waterproof results. Other printing technologies, such as MultiJet Modeling, would also meet the requirements. The anatomical shapes of the phantom are characterized by predominantly curved structures. This results in a limitation of the printability of very small components such as the vessels. For this reason, the caudal parts of the aorta and the vena cava had to be extended to an inner diameter of 1 mm. Nevertheless, the model mostly reflects the anatomical data in size and relative position.

After printing, it is necessary to flush out the resin remaining in the model. This has to be done immediately and in a dark environment. Afterwards, the phantom has to be post-cured. The model was further impregnated with Nano-Seal (JELN GmbH, Schwalmtal, Germany) to prevent the absorption of water. Eventually, the vessels, which were printed in two parts, were stuck together via the connection shown in Figure 1 (top right) using epoxy adhesive.

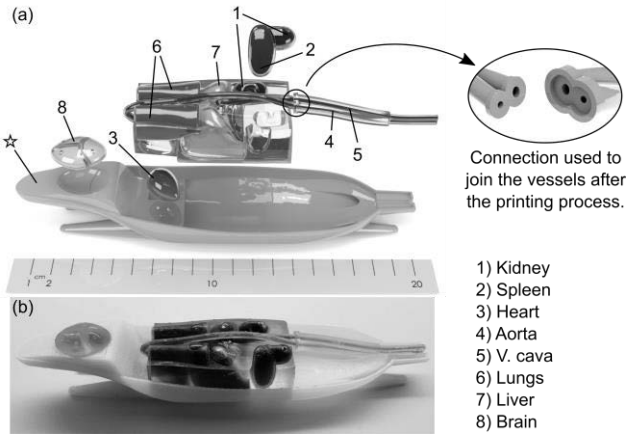

Figure 1: CAD model (a) and 3D printed and filled phantom (b). The entire model measures 203.5 mm × 45 mm × 36 mm. It mimics an 8-week-old rat of about 200 g.

The support skin (marked with ☆ in Figure 1a) has the shape of the lower half of the rat's body and guarantees a reproducible positioning of the organs. It was fabricated with the less expensive Ultimaker 3 (Ultimaker B.V., Geldermalsen, Netherlands), a 3D printer based on fused deposition modeling, as no waterproof printing is required.

2.3 MPI Measurement

For the MPI measurement, the organs and vessels of the model were filled with perimag (micromod, Rostock, Germany, prod. code: 102-00-132, plain surface) at different concentrations (see Table 1). The printed model filled with tracer is shown in Figure 1b. In order to determine the tracer concentrations of the individual organs and vessels, a steady state had to be assumed. When a tracer is injected into a living rat, it is distributed differently throughout the body over time. After the tracer is injected via the vena cava, it passes the heart and after a tracer-dependent blood half-live, it accumulates in certain organs such as the liver or spleen [6,7]. For the measurement, a state was assumed, in which the particles are distributed evenly in the blood without accumulation. Since each organ is supplied with blood to different degrees, the concentrations of the tracer were determined from the ratio of the blood volume contained in the respective organ [8] to the entire organ volume. The latter were derived from the CAD model. These values as well as the resulting tracer concentrations can be obtained from Table 1. The concentration in the heart was also used as the concentration for the vessels.

The measurements were performed using a 3D field free point preclinical MPI scanner (model: 1P MPI25/20 FF, Bruker, Ettlingen, Germany). For imaging, an excitation field amplitude of 12 mT in all three directions was applied.

Further, a selection field with a gradient strength of $\mathbf{G}$ = diag(-0.6, -0.6, 1.2) Tm^{-1} was used. The resulting FOV measures 40 × 40 × 20 mm^3. The phantom was moved along the x- and z-directions inside the scanner bore to 21 positions (7 × 1 × 3). The resulting region of interest (ROI) of 220 × 40 × 40 mm^3 covers the entire rat model. With this approach, issues connected to the usage of focus fields, such as field imperfections, could be neglected. Further, a single system matrix could be used for the reconstruction [9].

Due to the contrast limitations of the reconstruction, the large ratio of the highest to the lowest tracer concentration cannot be reconstructed within a single image. Therefore, the kidneys, the brain and the vessels were reconstructed separately by dividing the reconstruction into three parts along the longitudinal axis of the rat. The 6 patches at the first two x-positions were combined as well as the 9 patches at the middle three x-positions and 6 patches at the last two x-positions. The combined patches were reconstructed jointly solving one system of equations as proposed in [9]. An iterative regularized Kaczmarz algorithm [10] implemented in the open source programming language Julia was used as the solver. The reconstruction was performed with a relative regularization parameter of λ = 0.01, a signal-to-noise ratio (SNR) of 3 and 2 iterations.

Table 1: Overview of the organs and vessels with their volumes, the contained blood volume and the tracer concentrations used for the measurement.

Organ or vessel	Organ volume in the phantom [mm^3]	Mean blood volume in a living rat [mm^3] [8]	Tracer concentration [µg(Fe) ml^{-1}]
1) Kidney	495	450	2430
2) Spleen	318	140	1215
3) Heart	1488	490	810
4) Aorta	200	-	810
5) V. cava	590	-	810
6) Lungs	3610	660	486
7) Liver	14077	1660	270
8) Brain	1576	41	74

3 Results

The reconstruction results of all organs and vessels within a single image are shown in Figure 2. In the unwindowed image (a), all organs of the thoracic and abdominal region can be identified. However, the brain and the vessels are not visible due to the low tracer concentration of the brain compared to the kidneys and the small diameters of the vessels. In the image below (b), the display range was adjusted from 0 % to 10 % of the signal maximum of the reconstructed image. All higher values were set to the maximum value of the colorbar. While the brain and the vessels are visible, the other organs can no longer be distinguished. Besides, the artifacts become more prominent. In Figure 3 the results of the divided reconstruction are presented. The images were normalized to the respective maximum intensity. Additionally, the signal values below 10 %, 5 % and 25 % of the signal maximum of the respective part were set to zero. By separating the reconstruction, all organs and vessels could be successfully visualized.

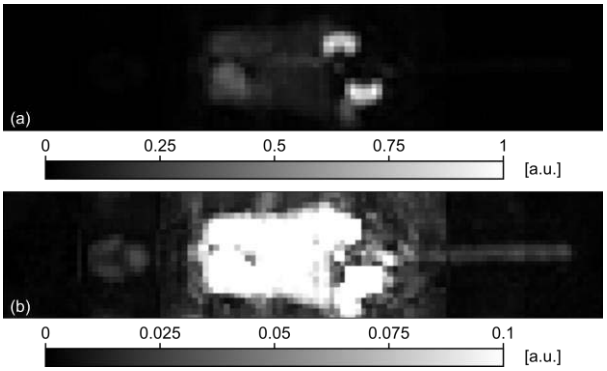

Figure 2: Reconstruction of all organs and vessels within a single image. The results are presented as maximum intensity projection in coronal view. In (a) the unwindowed image is shown. In (b) the display range is set between 0 and 10 % of the signal maximum of the reconstructed image.

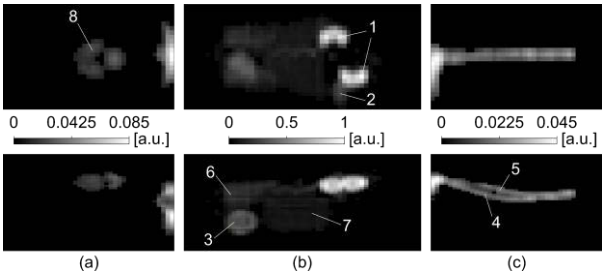

Figure 3: Division of the reconstruction into three parts. The results are presented as maximum intensity projection in coronal (top) and sagittal view (bottom). The head region (a), the thoracic and abdominal region (b) and the vessels (c) are shown.

4 Discussion and Conclusion

The presented phantom is based on an anatomy atlas and reflects the anatomy of the most important organs and vessels of the rat. These were selected with a view to typical experiments within the preclinical imaging field of MPI. In

the future, the model could be extended by further organs, such as the gastrointestinal tract, or tumor models.

The phantom can be used to evaluate medical procedures, plan and train experiments and animal handling before *in vivo* experiments and to compare *in vivo* images to phantom images of the same structure. The burden for animal studies can be reduced by using the model to determine the position of the entire rat as well as its organs and vessels in the FOV prior to an *in vivo* experiment and thus avoiding experiment failure due to a dispositioning. In addition, experimental procedures, sequences and algorithms can be tested in a realistic setup without the regulatory overhead that is necessary for animal studies.

Comparing the organ volume in the phantom with the mean blood volume in a living rat, the kidneys have a high blood content. Even if the kidneys of a living animal have a strong blood supply, the kidneys of the rats in the anatomy atlas used for the model creation are relatively small. However, the rat kidney can differ significantly in size [11].

The model was evaluated with MPI but could also be adapted for other imaging modalities using other tracers such as iodine or gadolinium. Furthermore, the data acquired from MRI measurements could be overlaid on the MPI images to analyze the resolution behavior within the phantom.

Physiological questions cannot be represented with the model. In addition, no dynamic experiments can be performed, since the model lacks a complete vascular system. Since MPI enables real-time imaging, a model that can plan and simulate dynamic *in vivo* experiments would enhance the possibilities of the phantom. For this purpose, the model could be extended by a more complex vascular system that connects the individual organs. Using a pump, a circulation could be established in the model.

The presented model is scalable. Using a printer with a sufficiently high resolution, even mouse phantoms could be realized. 3D printing offers further possibilities to develop even more realistic phantoms. Using recently presented flexible and transparent stereolithography resin, the elastic properties of the vascular system could be reflected. Lately, it was shown that using human cells, even a 3D printed beating heart can be realized [12].

A 3D printed anatomical model of a rat was demonstrated. The phantom is a close fit to a real anatomical structure of a rat. Only small adaptions had to be made to ensure the printability of the phantom. All organs and vessels of the phantom were successfully imaged using an MPI tomograph. The model has proven to enhance the experiment planning in advance to *in vivo* imaging. Due to the anatomy-like structure, many experiments in rodents can be evaluated in the phantom instead of a living animal. As rodents are the most commonly used animals in medical research, its anatomy was chosen for this first phantom. For large animals, the discussed problems in printing accuracy become less problematic, which in turn enables to design anatomical phantoms of larger animals in even higher accuracy.

Author Statement

Research funding: The authors thankfully acknowledge the financial support by the DFG (grant number KN 1108/2-1) and the BMBF (grant number 05M16GKA). Conflict of interest: Authors state no conflict of interest. Informed consent: Informed consent has been obtained from all individuals included in this study. Ethical approval: The research related to human use complies with all the relevant national regulations, institutional policies and was performed in accordance with the tenets of the Helsinki Declaration, and has been approved by the authors' institutional review board or equivalent committee.

References

[1] Taylor K, et al. Estimates for Worldwide Laboratory Animal Use in 2005. Altern Lab Anim 2008;36:327-342.
[2] European Commission. Commission Staff Working Document. Accompanying document to the Report from the Commission to the Council and the European Parliament. Seventh Report on the Statistics on the Number of Animals used for Experimental and other Scientific Purposes in the Member States of the European Union. 2013. Part 1/5.
[3] Russell WMS, Burch RL. The Principles of Humane Experimental Technique. London: Methuen; 1959.
[4] Hayakawa T, Iwaki T. A Color Atlas of Sectional Anatomy of the Rat. Tokyo: Adosuri; 2008.
[5] Gleich B, Weizenecker J. Tomographic imaging using the nonlinear response of magnetic particles. Nature 2005;435:1214-1217.
[6] Weizenecker J, et al. Three-dimensional real-time in vivo magnetic particle imaging. Phys Med Biol 2009;54:L1–L10.
[7] Khandhar AP, et al. Evaluation of PEG-coated iron oxide nanoparticles as blood pool tracers for preclinical magnetic particle imaging. Nanoscale 2017;9:1299–1306.
[8] Oeff K, König A. Das Blutvolumen einiger Rattenorgane und ihre Restblutmenge nach Entbluten bzw. Durchspülung. Bestimmung mit P^{32}-markierten Erythrocyten. Naunyn-Schmiedebergs Arch 1955;226:98-102.
[9] Szwargulski P, et al. Efficient Joint Image Reconstruction of Multi-Patch Data Reusing a Single System Matrix in Magnetic Particle Imaging. IEEE Trans Med Imaging 2019;38:932-944.
[10] Kaczmarz S. Angenäherte Auflösung von Systemen linearer Gleichungen. Bull Internat Acad Polon Sci 1937;*A35*:355–357.
[11] Treuting PM, et al. Comparative Anatomy and Histology. London: Academic Press; 2018.
[12] Noor N, et al. 3D Printing of Personalized Thick and Perfusable Cardiac Patches and Hearts. Adv Sci 2019;1900344.